A novel solution for an SDR-based anti-radiation seeker integrating CNN-based RF fingerprint recognition with DOA estimation

Le Van Bao*

Institute of Missile, Academy of Military Science and Technology, 17 Hoang Sam, Nghia Do, Hanoi, Vietnam.

*Corresponding author: baolehvpkkq@gmail.com

Received 15 Jun. 2026; Revised 20 Aug. 2026; Accepted 04 Sep. 2026; Published 16 Sep. 2026.

DOI: https://doi.org/10.54939/1859-1043.j.mst.FMC.2026.173-181

ABSTRACT

Anti-radiation seekers play an important role in passive detection and localization of hostile RF emitters. This paper proposes an SDR-based anti-radiation seeker architecture integrating convolutional neural network (CNN)-based RF fingerprint identification with MUSIC-based DOA estimation. Received I/Q signals are converted into normalized log-differential spectrograms for CNN-based emitter classification, while synchronized two-channel measurements provide spatial information for MUSIC processing. The two branches are combined to generate a joint emitter–direction output for target discrimination. A proof-of-concept experiment was conducted at 915 MHz using three transmitters configured with identical nominal frequency, bandwidth, transmit power, and waveform parameters. A total of 10,000 samples were collected across multiple acquisition sessions, of which 3,000 were held out for testing. The CNN achieved an overall classification accuracy of 90.37% with a mean confidence of 0.8775, while the MUSIC-based DOA estimator achieved a mean absolute angular error of 2.2518°. These results demonstrate the feasibility of combining RF fingerprint identification and spatial estimation within the proposed seeker-oriented SDR architecture under the tested conditions.

Keywords: Anti-radiation seeker; SDR; RF fingerprinting; CNN; DOA estimation; Emitter identification.

1. INTRODUCTION

Anti-radiation seekers are passive radio-frequency (RF) sensing systems designed to detect and track electromagnetic emitters without transmitting an interrogating signal. Their passive operation reduces seeker observability; however, it also limits the directly measurable target information. In particular, passive seekers primarily provide angular measurements, such as line-of-sight (LOS) direction and LOS rate, whereas target range and range rate are not directly available as in active or semi-active seeker configurations [1-3]. Reliable extraction of target-related information from received RF emissions is therefore a key requirement for passive seeker signal processing.

In practical electromagnetic environments, direction information alone may be insufficient for reliable target discrimination because multiple emitters can operate with similar nominal carrier frequencies, bandwidths, and waveform parameters. RF fingerprint identification (RFFI) provides an additional means of emitter discrimination by exploiting transmitter-specific hardware impairments introduced by RF components, including oscillator instability, carrier-frequency offset, and power-amplifier nonlinearities [5, 7]. Software-defined radio (SDR) is particularly suitable for this purpose because its center frequency, sampling rate, bandwidth, and digital signal-processing chain can be reconfigured for different RF operating conditions [4]. Recent studies have also demonstrated that time-frequency representations, particularly spectrograms combined with convolutional neural networks (CNNs), can effectively extract discriminative RF fingerprint features from received I/Q signals [6, 8, 9].

Direction-of-arrival (DOA) estimation provides complementary spatial information by exploiting the relative phase relationships among synchronized receiving channels. Among high-resolution subspace-based methods, MUSIC estimates the incident direction from the signal and

noise subspaces of the spatial covariance matrix and is widely used for array-based source localization [12, 13]. Recent studies have investigated SDR-based MUSIC direction estimation and tracking for rapidly moving RF emitters [14], as well as broadband source localization combining convolutional neural networks with coherent signal subspace methods [15]. Consequently, combining RF fingerprint recognition with DOA estimation enables a received signal to be characterized by both its emitter identity and spatial direction, providing more informative target discrimination than either function used independently.

This paper proposes an SDR-based anti-radiation seeker architecture integrating CNN-based RF fingerprint recognition with MUSIC-based DOA estimation. The CNN extracts transmitter-specific features from normalized log-differential spectrograms, while synchronized two-channel I/Q measurements are used by the MUSIC processing branch to estimate the corresponding arrival direction. The two outputs are associated to form a joint emitter–direction representation for seeker decision support. The proposed architecture is experimentally evaluated at 915 MHz using three transmitters configured with identical nominal transmission parameters. The main contribution of this work is the integration of reconfigurable SDR acquisition, CNN-based RF fingerprint classification, and spatial DOA estimation within a unified passive seeker-oriented processing framework. The present study is intended as a proof-of-concept validation of the proposed architecture rather than a complete operational anti-radiation seeker implementation.

2. PROPOSED SDR-BASED RF EMITTER IDENTIFICATION AND DOA ESTIMATION ARCHITECTURE

2.1. Overall architecture

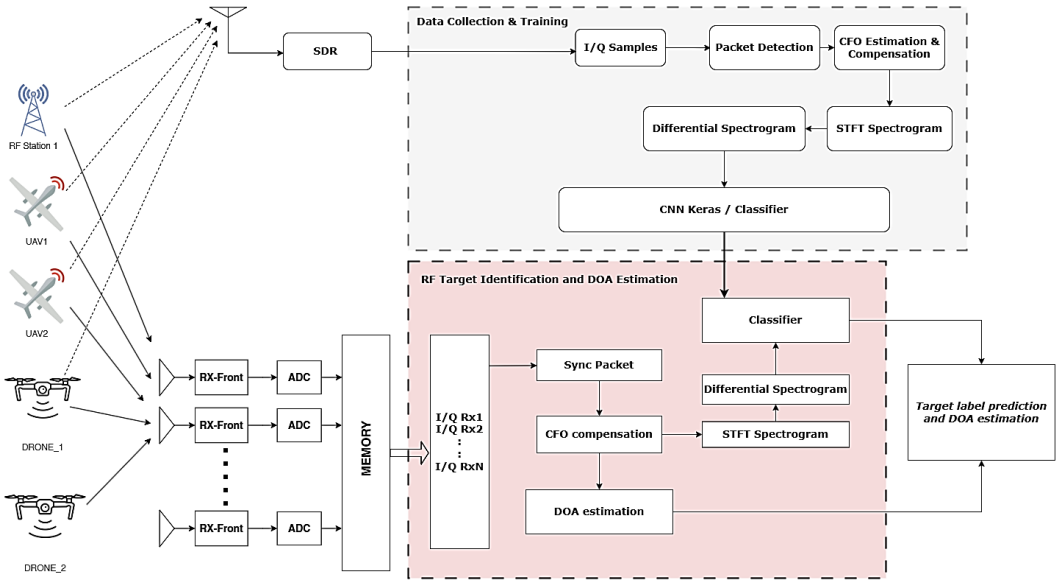


Figure 1. *Proposed SDR-based RF emitter identification and DOA estimation architecture.*

Figure 1 presents the proposed SDR-based architecture for RF emitter identification and DOA estimation, consisting of two main stages: offline data collection and CNN training, and online emitter identification and DOA estimation. In the offline stage, received RF signals are converted into complex baseband I/Q samples and processed through packet detection, amplitude normalization, CFO estimation and compensation, STFT, and log-differential spectrogram generation. The resulting normalized time–frequency representation is used to train the CNN to extract transmitter-specific RF fingerprint features associated with hardware-induced impairments rather than nominal signal parameters.

During online operation, synchronized multi-channel I/Q samples are processed using the same preprocessing chain to ensure consistency with the training data. The CNN outputs the predicted emitter label and classification confidence, while the MUSIC-based DOA branch forms the spatial covariance matrix, performs eigenvalue decomposition, constructs the noise subspace, and estimates the arrival angle from the peak of the MUSIC pseudo-spectrum. The two outputs are associated at the sample level to form a joint emitter–direction representation. This fusion provides both identity and spatial information, overcoming the limitations of using RF fingerprint classification or DOA estimation independently and supporting more reliable target discrimination in the proposed anti-radiation seeker architecture.

2.2. Signal preprocessing and CNN-based RF fingerprint recognition

The received complex baseband signal is modeled as [11]:

$$\boldsymbol{x}[n] = \boldsymbol{s}[n]e^{j(2\pi\Delta f n T_s + \phi)} + \boldsymbol{v}[n] \tag{1}$$

where $s[n]$ is the transmitted baseband signal, Δf is the carrier-frequency offset (CFO), T_s is the sampling interval, and $\boldsymbol{v}[n]$ denotes additive noise.

Packet synchronization is first performed to extract the useful signal segment. For a known preamble p[n], the correlation metric can be expressed as

$$\boldsymbol{C}[k] = \sum_{n=0}^{L-1} \boldsymbol{x}[k+n]p^*[n] \tag{2}$$

and the packet start index is estimated by $\hat{k} = \arg\max_k |\boldsymbol{C}[k]|$

The synchronized sequence is then corrected for the estimated CFO according to

$$\tilde{\boldsymbol{x}}[n] = \boldsymbol{x}[n]e^{-j2\pi\widehat{\Delta f} n T_s} \tag{3}$$

The compensated signal is transformed into the time-frequency domain using the short-time Fourier transform (STFT) [10]:

$$\boldsymbol{X}(m,k) = \sum_n \tilde{\boldsymbol{x}}[n]\boldsymbol{w}[n-mR]e^{-\frac{j2\pi kn}{N}} \tag{4}$$

where w[n] is the window function, m is the time-frame index, R is the hop size, k is the frequency-bin index, and N is the FFT size.

The spectrogram is obtained from the squared magnitude of the STFT:

$$\boldsymbol{S}(m,k) = |\boldsymbol{X}(m,k)|^2 \tag{5}$$

To suppress slowly varying spectral components and enhance local transmitter-dependent variations, the log-differential representation is defined as

$$\boldsymbol{D}(m,k) = \log\frac{\boldsymbol{S}(m,k)+\varepsilon}{\boldsymbol{S}(m-1,k)+\varepsilon} \tag{6}$$

where $\varepsilon > 0$ prevents numerical instability. To enhance the training stability of the CNN and ensure robust feature representation under varying channel conditions, the differential spectrogram is subsequently normalized using Z-score standardization as

$$\widehat{\boldsymbol{D}}(m,k) = \frac{\boldsymbol{D}(m,k)-\mu}{\sigma} \tag{7}$$

where μ and σ denote the mean and standard deviation of $\boldsymbol{D}(m,k)$, respectively. The standardized spectrogram $\widehat{\boldsymbol{D}}(m,k)$ is then resized to 64×64×1 before being applied to the CNN classifier. The proposed network consists of three convolutional layers with ReLU activation, generating 32, 64, and 48 feature maps, respectively. Two 2×2 max-pooling layers are placed after the first and second convolutional layers, followed by a fully connected layer with 96 neurons and a dropout

rate of 0.5. A three-class softmax layer produces the emitter-class probabilities. Figure 2 summarizes the complete preprocessing chain and the implemented CNN architecture.

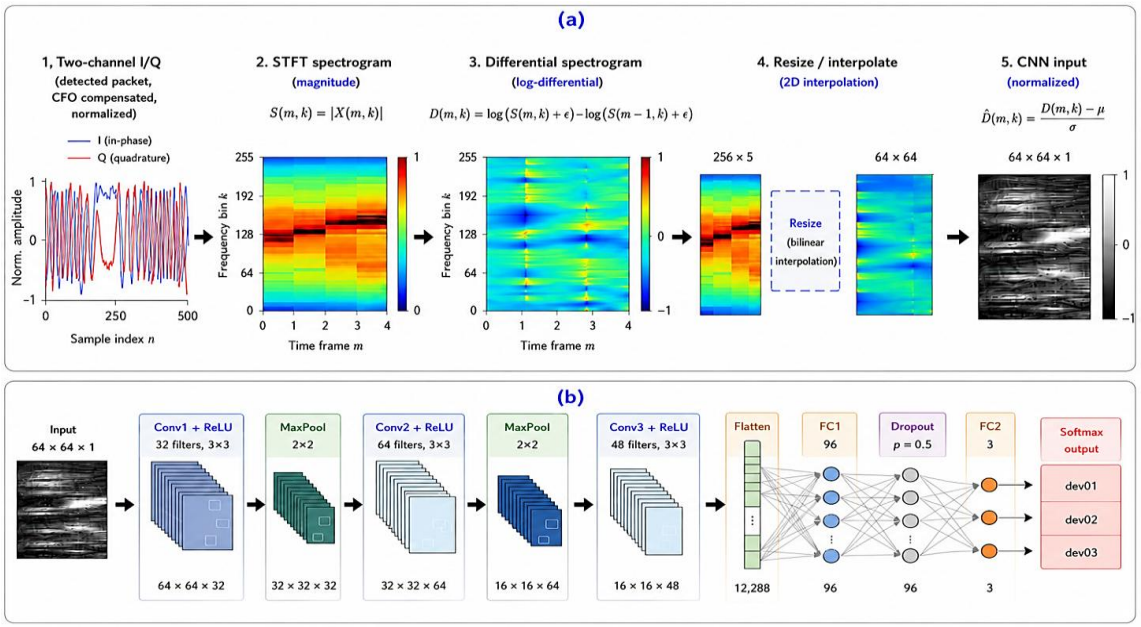


Figure 2. *Signal preprocessing and CNN architecture: (a) normalized log-differential spectrogram generation; (b) proposed CNN classifier.*

2.3. MUSIC-based DOA estimation from synchronized two-channel I/Q data

After synchronization and common reference complex gain calibration, the M-channel received signal is modeled as [14]:

$$\tilde{\boldsymbol{x}}[n] = \boldsymbol{a}(\theta)\boldsymbol{s}[n] + \boldsymbol{v}[n] \tag{8}$$

where $a(\theta)$ is the steering vector. For a uniform linear array

$$\boldsymbol{a}(\theta) = \left[1, e^{-j\frac{2\pi}{\lambda}d\,sin(\theta)}, e^{-j\frac{2\pi}{\lambda}2d\,sin(\theta)}, \dots, e^{-j\frac{2\pi}{\lambda}(M-1)d\,sin(\theta)}\right]^T \tag{9}$$

where d is the antenna spacing and λ is the wavelength. The spatial covariance matrix is estimated by

$$\boldsymbol{R}_{XX} = \frac{1}{N}\sum_{n=1}^{N}\tilde{\boldsymbol{x}}[n]\tilde{\boldsymbol{x}}^H[n] \tag{10}$$

After eigenvalue decomposition of $\boldsymbol{R_{XX}}$, the noise subspace matrix $\boldsymbol{E}_n$ is obtained. The MUSIC pseudo-spectrum is

$$\boldsymbol{P_{MUSIC}}(\theta) = \frac{1}{\boldsymbol{a}^H(\theta)\boldsymbol{E}_n\boldsymbol{E}_n^H\boldsymbol{a}(\theta)}, \hat{\theta} = \arg\max_{\theta}\boldsymbol{P_{MUSIC}}(\theta) \tag{11}$$

2.4. Fusion of RF fingerprint classification and DOA estimation

The CNN and MUSIC branches provide complementary identity and spatial information. For the i-th candidate, the CNN provides the classification confidence $\boldsymbol{p_i}$, while the DOA branch provides the spatial confidence $\boldsymbol{q_i}$. The fused decision score is defined as

$$\boldsymbol{J_i} = \alpha\boldsymbol{p_i} + (1-\alpha)\boldsymbol{q_i}, 0 \le \alpha \le 1 \tag{12}$$

where α controls the relative contribution of the two branches. α = 0.5 is used as a neutral weighting factor.

The final system output is represented as $y_{out} = (\hat{y}, \hat{\theta})$. This joint emitter–direction representation provides both identification and angular information for the final seeker decision.

3. RESULTS AND DISCUSSION

The experimental setup consisted of three RF transmitters (dev01–dev03), each implemented using a Semtech SX1262 RF transceiver, a synchronized two-channel bladeRF receiver, two receiving antennas, and an NVIDIA Jetson Orin Nano processing platform. All three transmitters were configured with identical nominal transmission parameters, including a center frequency of 915 MHz, a transmit power of 10 dBm, a signal bandwidth of 125 kHz, and the same channel and waveform settings. Therefore, the CNN classifier could not rely on these nominal parameters for emitter discrimination and instead had to exploit device-specific RF fingerprint characteristics contained in the received I/Q signals. Both bladeRF receiver channels were sampled synchronously at 2 MS/s. For DOA estimation, the two receiving antennas were arranged as a two-element uniform linear array with an inter-element spacing of d=λ/2. Prior to MUSIC-based spatial processing, common reference complex gain calibration was applied to compensate for residual inter-channel amplitude and phase mismatch and to improve phase coherence between the two receivers.

A total of 10,000 measured signal segments were collected over multiple independent acquisition sessions. Of these, 7,000 samples were used for training and validation and 3,000 were held out for testing. Each sample contained 512 complex I/Q samples and was converted by the same preprocessing chain into a normalized 64×64×1 log-differential spectrogram. The CNN was trained for 100 epochs using the Adam optimizer with an initial learning rate of 3×10^{-4}, sparse categorical cross-entropy loss, and a batch size of 32. ReduceLROnPlateau was employed to adapt the learning rate based on the validation loss, using a reduction factor of 0.5, a patience of 4 epochs, and a minimum learning rate of 10^{-5}.

The training behavior of the proposed CNN classifier is presented in Figure 3.

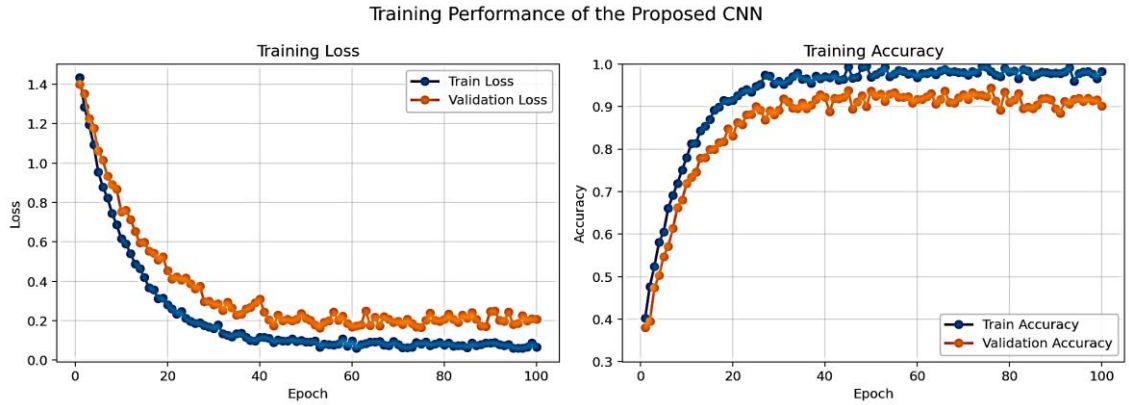


Figure 3. *Training and validation performance of the proposed CNN classifier.*

The training loss decreases rapidly during the first epochs and then gradually converges, showing that the network can learn discriminative RF fingerprint features from the input representation. At the final epoch, the training loss reaches 0.0665, while the validation loss reaches 0.2067. The training accuracy reaches 98.26%, whereas the final validation accuracy reaches 90.15%. The best validation accuracy observed during training is 94.42%.

Figure 4 presents the confusion matrix obtained from 3000 RF emitter detections. The classifier correctly identifies 903 samples of dev01, 907 samples of dev02, and 901 samples of dev03. Therefore, the total number of correct detections is

$$N_{correct} = 903 + 907 + 901 = 2711$$

The overall classification accuracy is calculated as

$$Acc = \frac{2711}{3000} = 90.37\%$$

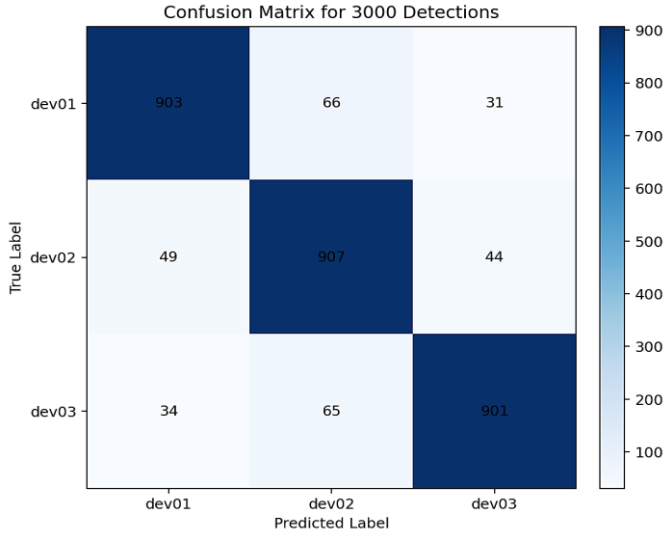


Figure 4. *Confusion matrix of RF emitter identification using 3000 measured samples.*

The confusion matrix shows that the proposed CNN classifier achieves comparable classification performance for all three emitters. The recall values of dev01, dev02, and dev03 are 90.30%, 90.70%, and 90.10%, respectively. This indicates that the proposed RF fingerprint representation provides balanced discriminative capability across the three devices. However, the main misclassification tendency occurs toward dev02. Specifically, 66 samples of dev01 and 65 samples of dev03 are incorrectly classified as dev02. This explains the over-detection of dev02 observed in the class distribution result.

The prediction confidence distribution is illustrated in Figure 5.

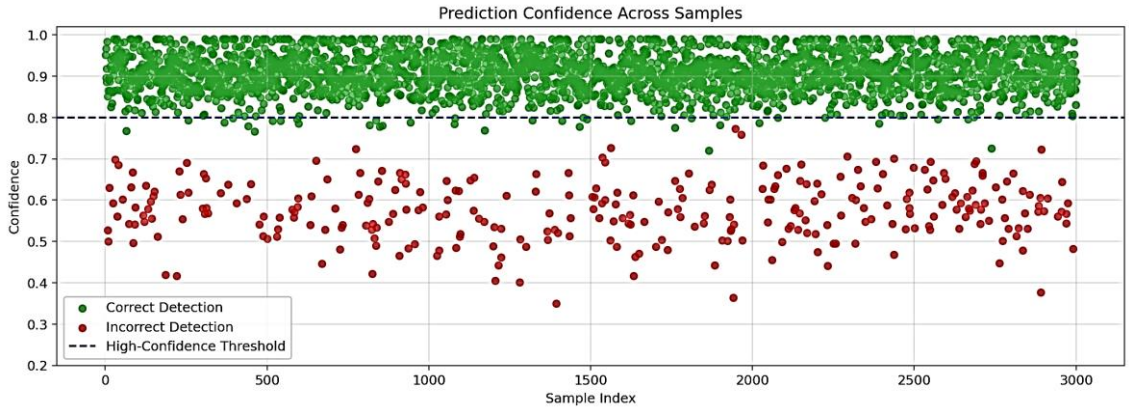


Figure 5. *Prediction confidence distribution of the CNN-based RF fingerprint classifier.*

Most correct detections are concentrated above the high-confidence threshold of 0.8, while most incorrect detections are distributed below this threshold. The mean prediction confidence over all samples is 0.8775, indicating that the CNN classifier generally produces reliable softmax outputs. This separation between correct and incorrect detections shows that the confidence score can be used as an additional reliability criterion in the final decision process.

A confidence-based rejection rule can be formulated as

$$\hat{y} = \begin{cases} arg\max_i p_i, \max_i p_i \geq \eta, \\ unknown, \max_i p_i < \eta \end{cases}$$

where $p_i$is the softmax probability of the i-th emitter class and η is the confidence threshold. In this work, η=0.8 is used as the high-confidence threshold. This rule can reduce false identification by rejecting low-confidence samples that are more likely to correspond to ambiguous RF fingerprints, noisy observations, or unstable channel conditions.

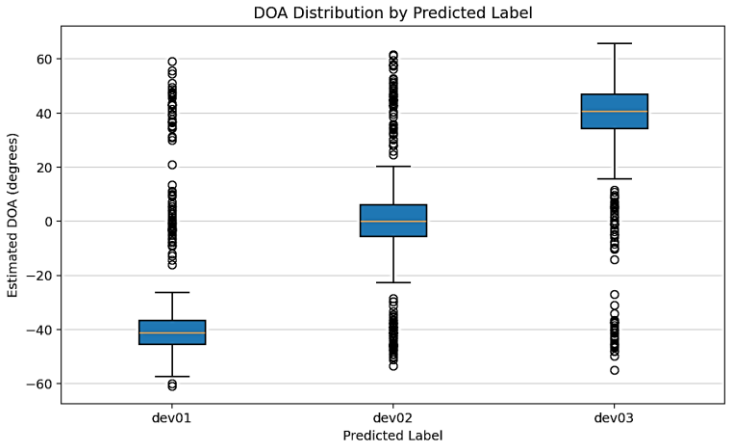


Figure 6. *Joint CNN–DOA output: DOA distributions grouped by CNN-predicted emitter labels.*

Figure 6 illustrates the joint CNN–DOA output by grouping the MUSIC-based DOA estimates according to the emitter labels predicted by the CNN. Most dev01, dev02, and dev03 samples are concentrated around their nominal angular regions of approximately −40°, 0°, and + 40°, respectively. Samples appearing in other angular regions, such as dev01-labeled samples near 0° or + 40°, indicate inconsistencies between emitter identification and angular estimation. These outliers may result from CNN misclassification, DOA estimation errors, or both, and therefore provide a direct visualization of the joint label–angle performance of the proposed fusion framework.

The MUSIC-based DOA estimator achieves a mean absolute error of 2.2518°. The remaining angular outliers may be attributed to low SNR, residual CFO, inter-channel phase mismatch, multipath propagation, or ambiguity associated with the two-antenna configuration. Figure 6 further highlights the joint CNN–DOA behavior by revealing cases where the predicted emitter label is inconsistent with the corresponding estimated direction, thereby providing a direct visualization of label–angle inconsistencies in the proposed fusion framework.

Overall, the experimental results demonstrate that the proposed SDR-based framework can jointly perform RF emitter identification and DOA estimation. The CNN classifier provides emitter-level discrimination based on RF fingerprint features, while the two-channel DOA estimation block provides spatial information from the received phase difference. The final output of the system can therefore be represented as $(\hat{y}, \hat{\theta})$, where $\hat{y}$ is the predicted RF emitter label and $\hat{\theta}$ is the corresponding estimated direction of arrival.

4. CONCLUSIONS

This paper proposed a low-cost SDR-based anti-radiation seeker architecture integrating CNN-based RF fingerprint recognition with MUSIC-based DOA estimation. The proposed approach combines emitter-specific information extracted from received RF signals with spatial information

obtained from synchronized two-channel I/Q measurements, enabling joint emitter identification and direction estimation within a unified seeker-oriented processing framework.

The proof-of-concept experiment was conducted at 915 MHz using three RF transmitters with identical nominal waveform parameters. Using 3,000 independent test samples, the CNN classifier achieved an overall classification accuracy of 90.37% with a mean prediction confidence of 0.8775, while the MUSIC-based DOA estimator achieved a mean absolute angular error of 2.2518°. These results demonstrate the feasibility of the proposed architecture for simultaneously identifying RF emitters and estimating their corresponding directions under the tested conditions.

Compared with using RF fingerprint recognition or DOA estimation independently, the proposed CNN–DOA fusion provides complementary identity and spatial information. The joint emitter–direction representation allows the system to associate each predicted emitter with its corresponding estimated arrival direction and also reveals cases in which the predicted identity is inconsistent with the estimated angular region. This capability provides additional information for target discrimination and decision-making in anti-radiation seeker applications.

The present work represents an initial proof-of-concept under static laboratory conditions rather than a complete validation of an operational anti-radiation seeker. Future work will focus on improving the robustness and generalization of the proposed architecture through experiments at different frequency bands, SNR levels, distances and transmitter positions, as well as under interference, multipath, simultaneous-emitter and dynamic operating conditions.

REFERENCES

[1]. N. F. Palumbo, "*Guest Editor's Introduction: Homing Missile Guidance and Control*", Johns Hopkins APL Technical Digest, Vol. 29, No. 1, pp. 2–11, (2010).

[2]. S. K. Güvenç, "*Range To-Go Estimation for a Tactical Missile with a Passive Seeker*", M.S. Thesis, Department of Aerospace Engineering, Middle East Technical University, Ankara, Turkey, (2015).

[3]. B. C. Babaoğlu, "*A Method for Estimating Target Velocity and Range with Passive Seeker Data*", M.S. Thesis, Department of Aerospace Engineering, Middle East Technical University, Ankara, Turkey, (2018).

[4]. J. Mitola, "*Software Radios: Survey, Critical Evaluation and Future Directions*", IEEE Aerospace and Electronic Systems Magazine, Vol. 8, No. 4, pp. 25–36, (1993).

[5]. G. Shen, J. Zhang, A. Marshall, L. Peng and X. Wang, "*Radio Frequency Fingerprint Identification for LoRa Using Spectrogram and CNN*", Proceedings of IEEE INFOCOM 2021 - IEEE Conference on Computer Communications, pp. 1–10, (2021).

[6]. S. Luo, "*Deep Learning Based RFF Identification for LoRa*", Teaching Demonstration, King's College London, (2020).

[7]. G. Shen, J. Zhang, A. Marshall and J. Cavallaro, "*Towards Scalable and Channel-Robust Radio Frequency Fingerprint Identification for LoRa*", IEEE Transactions on Information Forensics and Security, Vol. 17, pp. 774–787, (2022). DOI: 10.1109/TIFS.2022.3152404.

[8]. I. Goodfellow, Y. Bengio and A. Courville, "*Deep Learning*", MIT Press, Cambridge, MA, USA, (2016).

[9]. Y. LeCun, Y. Bengio and G. Hinton, "*Deep Learning*", Nature, Vol. 521, pp. 436–444, (2015).

[10]. A. V. Oppenheim and R. W. Schafer, "*Discrete-Time Signal Processing*", 3rd ed., Pearson, Upper Saddle River, NJ, USA, (2010).

[11]. S. Haykin, "*Communication Systems*", 4th ed., John Wiley & Sons, New York, NY, USA, (2001).

[12]. R. O. Schmidt, "*Multiple Emitter Location and Signal Parameter Estimation*", IEEE Transactions on Antennas and Propagation, Vol. AP-34, No. 3, pp. 276–280, (1986).

[13]. H. L. Van Trees, "*Optimum Array Processing: Part IV of Detection, Estimation, and Modulation Theory*", Wiley-Interscience, New York, NY, USA, (2002).

[14].L. V. Bao, N. Q. Vinh, and P. C. Tu, *"Direction estimation and tracking of rapidly moving RF emitters",* Journal of Military Science and Technology, vol. 107, no. 107, pp. 3–12, (2025), doi: 10.54939/1859-1043.j.mst.107.2025.3-12.

[15].N. T. Thien, H. H. Cuong, T. Q. Hien, N. M. Hung, and D. D. Dien, *"Broadband signal source localization using convolutional neural networks combined with coherent signal subspace methods",* Journal of Military Science and Technology, no. IITE, pp. 115–122, (2025), doi: 10.54939/1859-1043.j.mst.IITE.2025.115-122.

TÓM TẮT

Giải pháp đầu tự dẫn chống bức xạ dựa trên vô tuyến định nghĩa bằng phần mềm (SDR) tích hợp nhận dạng dấu vân tay RF bằng mạng CNN với ước lượng hướng đến

Đầu tự dẫn chống bức xạ là một bộ phận quan trọng trong phát hiện và định vị thụ động các nguồn phát RF đối phương. Bài báo đề xuất kiến trúc đầu tự dẫn chống bức xạ dựa trên vô tuyến định nghĩa bằng phần mềm (SDR), tích hợp nhận dạng dấu vân tay RF bằng mạng nơ-ron tích chập (CNN) với ước lượng hướng đến (DOA) dựa trên thuật toán MUSIC. Các tín hiệu I/Q thu được được chuyển đổi thành ảnh phổ thời gian–tần số vi sai logarit đã chuẩn hóa để thực hiện phân loại nguồn phát bằng CNN, trong khi các phép đo đồng bộ từ hai kênh thu cung cấp thông tin không gian phục vụ xử lý MUSIC. Hai nhánh xử lý này được kết hợp nhằm tạo ra đầu ra liên hợp nguồn phát–hướng đến, phục vụ phân biệt mục tiêu. Một thí nghiệm kiểm chứng nguyên lý được tiến hành tại tần số 915 MHz, sử dụng ba bộ phát được cấu hình với cùng các tham số danh định về tần số, băng thông, công suất phát và dạng sóng. Tổng cộng 10.000 mẫu được thu thập qua nhiều phiên đo độc lập, trong đó 3.000 mẫu được tách riêng để sử dụng cho tập kiểm thử. Mô hình CNN đạt độ chính xác phân loại tổng thể 90,37%, với độ tin cậy trung bình 0,8775, trong khi bộ ước lượng DOA dựa trên MUSIC đạt sai số góc tuyệt đối trung bình 2,2518°. Các kết quả này chứng minh tính khả thi của việc kết hợp nhận dạng dấu vân tay RF với ước lượng không gian trong kiến trúc SDR định hướng ứng dụng cho đầu tự dẫn chống bức xạ được đề xuất, trong phạm vi các điều kiện thử nghiệm đã khảo sát.

Từ khóa: Đầu tự dẫn chống bức xạ; Vô tuyến định nghĩa bằng phần mềm; Nhận dạng dấu vân tay RF; Mạng nơ-ron tích chập; Ước lượng hướng đến; Nhận dạng nguồn phát.